Phase 1 Final Technical Report

Mohit Bhatia and Peter McIntyre
Accelerator Technology Corporation
9701 Valley View Dr.
College Station, TX 77845

MgB_2 Synthesis: Pushing to High Field

Accelerator Technology Corp. (ATC) has successfully completed its Phase 1 effort to develop rf plasma torch synthesis of MgB_2 superconducting powder. The overall objective is to develop a way to introduce homogeneous alloying of C and SiC impurities into phase-pure MgB_2. Several groups have attained remarkable benefits from such alloying in raising the upper critical field H_{c2} from ~14 T to ~30 T (bulk) and ~50 T (thin films). But *no one* has succeeded in producing that benefit homogeneously, so that current transport in a practical powder-in-tube (PIT) conductor is largely the same as without the alloying.

ATC has conceived the possibility of attaining such homogeneity by passing aerosol suspensions of reactant powders through an rf plasma torch, with each reactant transported on a streamline that heats it to an optimum temperature for the synthesis reaction. This procedure would uniquely access non-equilibrium kinetics for the synthesis reaction, and would provide the possibility to separately control the temperature and stoichiometry of each reactant as it enters the mixing region where synthesis occurs. It also facilitates the introduction of seed particles (*e.g.* nanoscale SiC) to dramatically enhance the rate of the synthesis reaction compared to gas-phase synthesis in rf plasma reported by Canfield and others.

During the Phase 1 effort ATC commissioned its 60 kW 5 MHz rf source for a manufacturing-scale rf plasma torch. This effort required repair of numerous elements, integration of cooling and input circuits, and tuning of the load characteristics. The effort was successful, and the source has now been tested to ~full power.

Also in the Phase 1 effort we encountered a subsidiary but very important problem: the world is running out of the only present supply of phase-pure amorphous boron. The starting boron powder must be in the amorphous phase in order for the synthesis reaction to produce phase-pure MgB_2. Even small contamination with crystalline boron results in the formation of parasitic phases such as MgB_4, MgB_7, *etc*. Such parasitic phases are a primary element of the connectivity problem, in which even though a sample powder may contain grains of high-quality MgB_2, adjacent grains are surrounded by intergrowths of parasitic phases so that current transport is badly degraded.

The best results to date have been obtained using boron powder produced long ago for a rocket propellant development project. The synthesis process was complex and is now largely lost, and the manufacturing equipment has long since been scrapped. The last batch of the powder has been used during recent years to support MgB_2 R&D at several labs, but supplies are dwindling.

ATC has identified a first application of its plasma torch to synthesize phase-pure amorphous boron flake using a rapid-quench splat technique. Inexpensive technical-grade boron would be purified of contaminants, then dispersed as an aerosol in inert gas and passed through the plasma torch to melt it into a spray. The spray would be splat-condensed on a rotating drum to form pure amorphous flake.

The process would begin with technical-grade boron powder, having good stoichiometric purity, nanoscale particles, but significant contamination of MgO and crystalline boron. We used wet chemistry to remove B_2O_3 completely and reduced the MgO impurity, and analyzed the particle size distribution using a Coulter counter and the phase composition using X-ray diffraction (XRD). The next step will be to build an rf plasma torch with a recirculating single-component aerosol feed and the cooled splat drum and collector, and undertake process development for amorphous boron powder.

This revised goal has two benefits. First, it is an easier technology than our ultimate goal of a multi-component laminar flow torch. We have been counseled by those experienced in plasma torch technology that our ultimate goal will require a torch that *should* be feasible but has never been attempted. It may require an extended period of R&D for both the torch itself and the gas dynamics in the reaction region.

Second, this simpler single-component process will yield a product powder that is important today for the many groups undertaking powder-metallurgy routes to MgB_2. The above success and learning curve has brought us to a significant shift of strategy from what was originally set out in the Phase 1 plan. But this shift has brought us to within sight of a powder product that will itself be an enabling boost for the community of MgB_2 developers.

Table of Contents

Success in the Phase 1 effort

ATC successfully completed two major goals of the Phase I program: we commissioning the 60kW 5MHz Lepel rf power generator for manufacturing-scale rf plasma torch synthesis; and we identified a first application of our plasma torch synthesis procedure to manufacture phase-pure amorphous boron, a key ingredient for high-performance MgB_2 for which there is currently no commercial source.

Commissioning of the rf power generator

ATC made a considerable initial investment and purchased a recent-model (used) Lepel generator, model no. T-60-3MC5-TLSP (Figure 1), configured for driving an rf plasma torch. This powder generator was tested configured and commissioned during the present Phase 1.

The initial testing included the visual inspection followed by detailed shorts and continuity testing, especially on the vacuum tube (Figure 2) and capacitor banks. Some of the parts were damaged (high-power resistors) during the shipping of the rf generator and were replaced.

The rf generator was connected to a 230 gallon low conductivity water tank with a 5 hp recirculating pump. An Advantage portable chiller with a 2 hp recirculation pump was also connected in-line to maintain the water temperature at 55 F for cooling the rf generator.

The rf generator was connected to 480V 3ϕ 180A input and is rated to generate 60 kW at 5MHz. The testing of the generator was performed with the recommended dummy load shown in Figure 3.

Figure 1. ATC's rf generator, commissioned and operational.

Figure 2. Vacuum tube in the rf generator during the test run.

Figure 3 Test load coil for rf generator.

Figure 4. rf generator in operation. 60kW plate output.

The test load is a 5" water-cooled coil made using copper tube. The load was cooled using city water. Two temperature gauges and a flowmeter were attached at the inlet and outlet of the water flow as shown in Figure 2. The power output of the rf generator was tested using the heat transferred to the water in the coil by measuring the temperature rate of rise. Figure 4 shows the panel meters on the rf generator indicating 60 kW output generated at the plate.

Materials science to support high-field performance MgB_2

Remarkably high H_{c2} in MgB_2 thin films has been achieved by various research groups by homogenous doping of C. There remains a major challenge for achieving comparable performance in strands and bulk samples. The main reason is that, while thin films can be synthesized with good homogeneity in composition and with reasonable control of intergrowths, bulk synthesis using powder metallurgy typically results in inhomogeneity in stoichiometry and intergrowths of parasitic phases, which in turn results in poor connectivity in the strands when the powder is incorporated into a powder-in-tube conductor. This inhomogeneity in the final product arises from either non-uniform mixing of the dopants or from the formation of non-superconducting parasitic phases like MgB_4, MgB_7, Mg_2B_{25}, *etc*. [1-4] which form because of incomplete reaction. One of the reasons for the latter is directly related to the fact that as compared to amorph-

ous boron, the crystalline boron which is in most of the cases the β-rhombohedral phase has a lower reactivity and thus limits Mg diffusion. Since, the formation reaction of MgB_2 involves inward diffusion of Mg in B and reaction at the interface, the slow diffusivity and lower reactivity leads to the formation of leftover intermediate non-superconducting phases at grain boundaries. This has been observed by various research groups [2, 3, 5]. It is widely accepted that high H_{c2}s and best performances are achieved in MgB_2 strands that are prepared using high purity amorphous boron as the starting raw material. A more detailed discussion on the differences between amorphous and crystalline boron starting powder is given in Appendix A.

ATC's rf-plasma synthesis method is aimed at ultimately achieving the uniform phase formation in doped MgB_2. But the present shortage of high-purity amorphous boron has led us to identify a first opportunity for our rf plasma process to produce phase-pure amorphous boron as a first product. The process would involve melting the boron particles suspended in an aerosol using our inductively coupled plasma torch and then splat-quenching them in the reaction chamber, followed by jet-milling and particle size separation.

During the Phase I effort we identified a technical grade boron powder obtained from Micron Metals as our starting raw material for the process. The powder is 90-95% pure and the major impurities include B_2O_3 and MgO. The particle size analysis on this powder was performed using a Coulter counter and is shown in Figure 5. As can be seen most of the particles are below 4 μm, which is beneficial because smaller particles would be faster to melt and quench and hence uniformly amorphous boron could be obtained with higher throughput.

Compositional analysis of the boron powder as provided by the vendor is shown in Table 1. The water soluble boron is essentially B_2O_3. The magnesium impurity is present in form of oxide (MgO). This was confirmed by performing the XRD analysis shown in Figure 6.

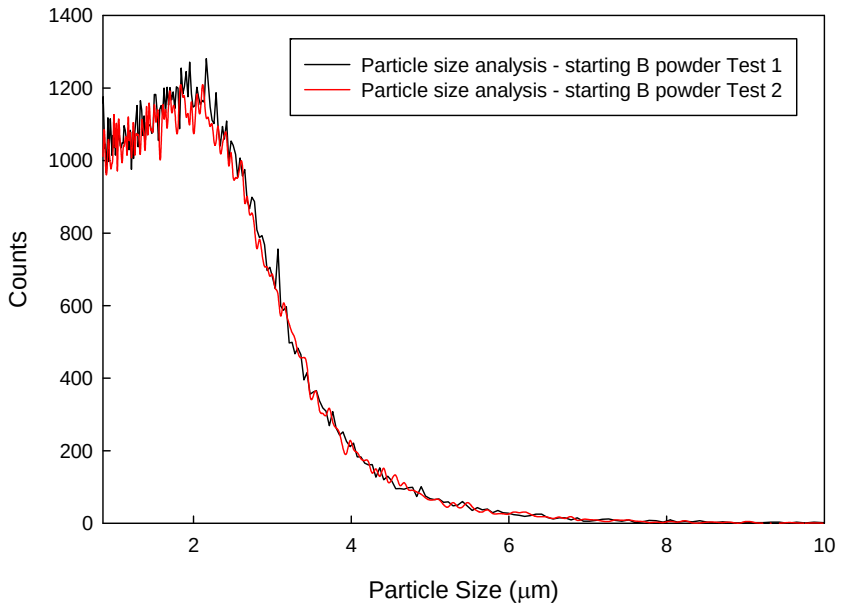

Figure 5. Particle size analysis on technical grade boron powder

Table 1. Compositional analysis of Micron Metals technical-grade boron powder.

Constituents	%
Boron	91.06
Magnesium	3.43
Insoluble in H_2O_2	0.73
Water Soluble Boron	0.59
Volatile Matter	0.33
Moisture	0.25

We developed a wet chemistry process to remove B_2O_3 from the starting materials and highly reduce the MgO content. The boron powder was mixed in conc. HCl, followed by separations of the boron particles using glass-fiber filter paper. The product powder was dried in an oven for 12 hrs at 120 C. A yield of 85% by weight was achieved in the process.

XRD was performed in the powder after this cleaning and is shown in Figure 6. The black curve in the figure shows the high-purity boron powder that was produced about 15 years back on a special order for the rocket propellant development project and is no longer available. To the best of our knowledge, this boron was produced by the decomposition of diboranes which is a very expensive and dangerous process. This boron has given some of the best performance in MgB_2 strands reported so far. The red curve shows the as-received boron powder from Micron Metals, and can be seen to contain MgO, B_2O_3, and crystalline boron as major impurities. The curve in green shows the state of the powder after it was cleaned by the process described above. It can be noticed that with our wet chemistry we have been able to successfully clean the starting powder of both impurity oxide phases, leaving almost pure boron (amorphous + crystalline).

We also prepared MgB_2 bulk samples by stoichiometrically mixing the B powder with Mg flake followed by powder compaction and sintering. MgB_2 samples were prepared using the technical-grade B as-received, and also using the technical-grade B after oxide removal. used a vibrating sample magnetometer (VSM) to measure the magnetization and then converting the measured ΔM into a critical current density, $J_{c,m}$, using Bean's model[6].

Figure 7 shows the variation of magnetic $J_{c,m}$ *vs*. applied field, B, for the two samples. It can be confirmed from this graph that the chemical cleaning did no harm in terms of the superconducting properties. It should be emphasized that this is just a preliminary result and it should be understood that no optimization of stoichiometry or heat-treatment was performed, and no attempt was made to introduce alloying with either C or SiC to enhance H_{c2}. Also, this powder still contains crystalline boron.

Following our success in cleaning the technical grade boron, we plan to use the cleaned boron to prepare pure, amorphous boron using our rf-plasma synthesis. The product of that development will then be available to be used by us and other researchers to produce homogeneous C/SiC doped MgB_2 with high H_{c2}.

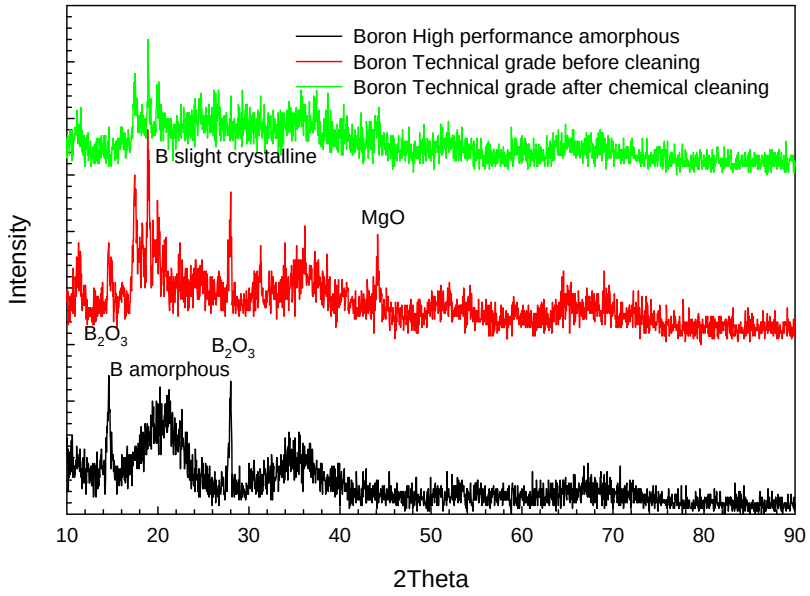

Figure 6. XRD analysis on three samples of boron powder: a) high-performance amorphous powder; b) technical-grade powder as supplied; c) technical-grade powder after oxide removal.

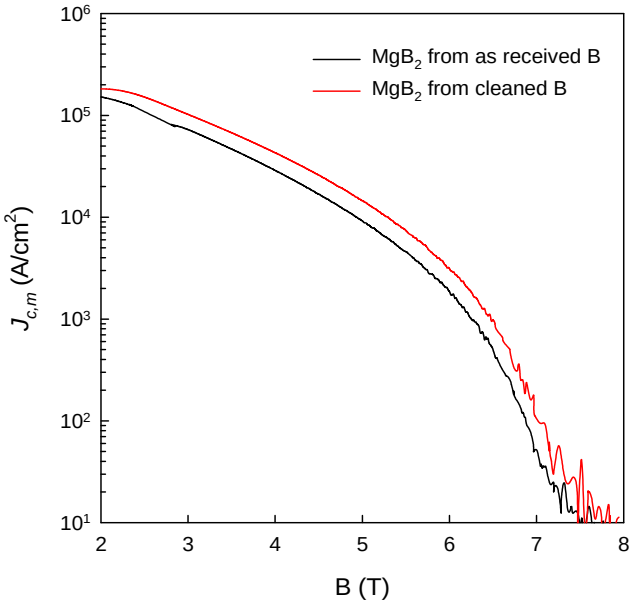

Figure 7. $J_{c,m}$ *vs.* B comparison for MgB_2 powder samples prepared from technical-grade boron powder: a) as-received powder; b) after oxide removal.

Plasma torch synthesis

Many research groups have tried various methods to enhance the upper critical field, H_{c2}, and hence produce high-performance MgB_2 superconductor. Caplin *et al.* [7] tried proton irradiation introduced atomic disorder and achieved increased irreversibility fields, H_{irr}, while Dou *et al.*, have achieved SiC and C (nanotubes) addition using powder metallurgy route and have reported a significant increase in H_{c2}.Wilke [8] and Orimichi [9] have shown that carbon doping can strongly enhance the parallel critical field in single crystal to about 33 T at 4 K. Braccini *et al.*[10], have attained values of about twice these values. C-doping was common to these highest H_{c2} films. A common underlying factor to achieving very high-performance MgB_2 is to be able to make highly homogeneous product with uniform doping of C/SiC. Canfield *et al.*, in their work, achieved this by introducing C and B as gaseous ingredients into an rf plasma torch, and the gas-phase reaction produced a small quantity of nanoscale flake of C-doped B with homogeneous stoichiometry of C doping. This success was compromised (in our view) by the subsequent attempt to react Mg with the C-doped B in a conventional powder metallurgy route. This step left un-reacted Mg at the grain boundaries and formed a variety of secondary phases instead of only the desired homogeneous one. We have conceived a particular approach to synthesis using rf-plasma that builds upon the work of Canfield.

We have proposed instead to introduce B and Mg as powders, each dispersed as an aerosol in an inert buffer gas, on separate streamlines in the inlet flow to an rf plasma torch. C will be introduced as a gaseous hydrocarbon on a third streamline.

This approach takes maximum advantage of the spatial temperature profile in the plasma and the possibility to introduce reactants at opportune locations in the longitudinal development of the plasma plume. The B and Mg would each be vaporized and the hydrocarbon would be dissociated as they pass through the plasma region, and since they are captured in laminar flow on separate streamlines they would each be heated to a temperature corresponding to that location in the plasma cross section. By choosing which streamline to inject each reactant we can control the individual temperatures that each are heated to prior to reaction.

One final ingredient will be injected on a cooler streamline: an aerosol dispersion of a nanoscale powder of a suitable material to serve as seeds for the synthesis reactions to be initiated in the exhaust plume. Appropriate choices for seeds are SiC, C fullerenes or nanotubes, and B_4C, all of which are available as nanoscale powders.

The synthesis reaction will then be initiated in the plume by introducing turbulent mixing as the exhaust plume leaves the plasma region and enters the reaction chamber. The rate of synthesis will be enhanced and the final grain size distribution controlled by seeding the synthesis reaction on the seed nanoparticles that passed through the torch region un-vaporized.

Starting with powder ingredients and vaporizing them opens the way to using the least expensive forms of the feed ingredients: B in the form of amorphous boron powder (~$50/kg) and the Mg in the form of flake (~$20/kg). This approach makes possible a remarkable degree of control over the separate temperatures of each reactant species, a seeding of crystal growth in the exhaust flow, and a control of the temperature-time profile that enables optimization of reaction kinetics and control of grain size distribution.

Even though this technique would lead to production of high performance MgB_2 and other non-equilibrium phase we have revised our plan for further development in light of the reality

that operation with multiple aerosol flows would require designing and building a torch that has never been attempted. While this remains our ultimate goal, we have identified synthesis of phase-pure amorphous B as our first implementation of the plasma torch synthesis and utilizing this high purity amorphous B as a starting material for preparation on MgB_2 using solid-state reaction route as the first approach.

As mentioned in the earlier section, the shortage of phase-pure amorphous B is a major concern for the MgB_2 development and production community and success in this more modest first process plan should enable us to supply high-priority amorphous B to MgB_2 developers and manufacturers at affordable prices. The ultimate goal of the project still remains to develop the direct synthesis route for homogeneous multi-component C doped MgB_2 and the success of the first process development will facilitate this goal.

Design for plasma torch

First attempt at splat-melt synthesis of amorphous B flakes

We plan a first attempt at the synthesis of amorphous B flakes using splat-melt synthesis. The work will be carried out using a DC plasma torch at SUNY Stony Brook in collaboration with Prof. Sanjay Sampath. Process development would be carried out to examine the role of process variables on the properties of B flakes formed. Effects of starting particle size, temperature, oxygen content, and velocity would be studied to find the optimum parameters which can then be used as the starting point for the design of our procedure using rf plasma torch. Deposition rate test would provide important insights in order to design our torch for high volume production.

Design of plasma torch synthesis for pure-amorphous boron synthesis

An rf plasma torch consists of a annular quartz tube assembly in which a gas passes through a region where an intense rf field is produced by inductive coupling. The rf field ionizes gas atoms and heats the ions and electrons to form a plasma, as shown in Figure 8. The plasma temperature can be controlled by the balance of gas flow rate and rf power, and it typically increases from ambient at the outer wall to ~5000 K at the hottest location in the flow. Figure 8 also shows a simulation of temperature profile and gas flow in the same rf plasma torch, as simulated by Mellado-Gonzalez *et al.*[11].

The first step in building a plasma torch is to design and simulate the torch. We have modeled the inductively coupled plasma torch using the commercially available fluid-flow modeling software, FLUENT and its magnetohydrodynamic (MHD) module [12, 13].

We have developed a 3-D model, similar to Figure 9c [12, 13], using GAMBIT (designing and mesh generation) for simulating the behavior of inductively coupled plasma torch (ICPT) under our synthesis parameters. The 2D model and dimensions of the most commonly used Tekna plasma torch (PL-50) design are shown in Figure 9 a, b. The helical coil is taken into account in its actual 3-D shape to include the effects of breaking axisymmetry on the plasma discharge. Steady state, continuity, momentum and energy equations would be solved for boron aerosol in argon optically thin plasmas under the assumptions of LTE and laminar flow. The electromagnetic field is obtained by solving the 3-D vector potential equation on a grid extending outside the torch region, Figure 9c. Modeling and designing the torch in such a way would help finalize various parameters involved in building the actual torch for our synthesis route.

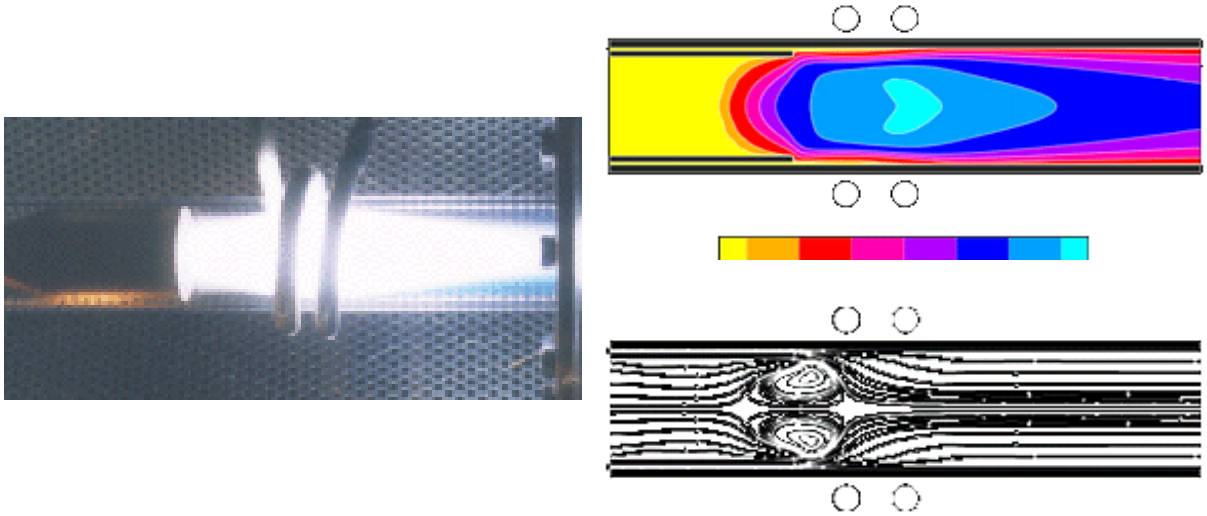

Figure 8. Simple RF plasma torch in operation. Profiles show temperature and velocity distributions in the plasma flow

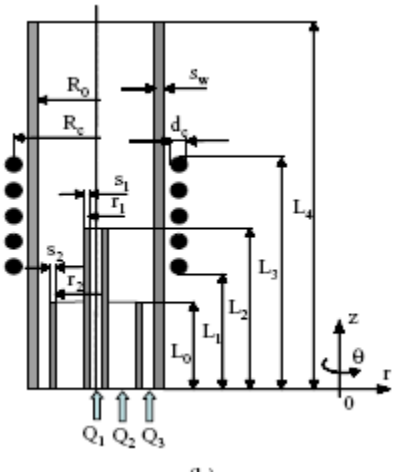

$r_1 = 1.7$ mm	$R_0 = 25$ mm
$r_2 = 18.8$ mm	$R_c = 33$ mm
$s_1 = 2$ mm	$d_c = 6$ mm
$s_2 = 2.2$ mm	$s_w = 3.5$ mm
$L_0 = 40$ mm	$L_3 = 110$ mm
$L_1 = 50$ mm	$L_4 = 170$ mm
$L_2 = 80$ mm	

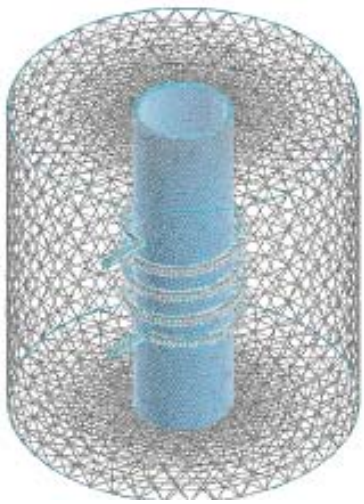

Figure 9. a) 2D model of Tekna PL-50 plasma torch, b) dimensions and c) 3D and mesh for Tekna Pl-50 plasma torch

Building the rf plasma torch and integrate with power supply and ATC's aerosol system

We plan to build the rf plasma torch based on these optimized parameters for processing a ingle component system. The torch would be water cooled and would have single central inlet for the aerosol powder. One of the major challenges in building a rf torch is the design of the rf coupling coil. The pitch angle, number of turns and the positioning of the coil directly influence the symmetry and the temperature of the plasma plume. The rf coil would be designed to obtain a axis symmetric plume for obtaining about 2700 K at the center. Figure 10 shows the design of a simple single component rf plasma torch.

The plasma torch would be integrated with the power supply and tuned for the optimized power coupling. The system would also be integrated with ATC's aerosol system where in the previously chemically cleaned technical grade boron powder would be suspended in Argon as aerosol to be used as an input for the plasma synthesis method.

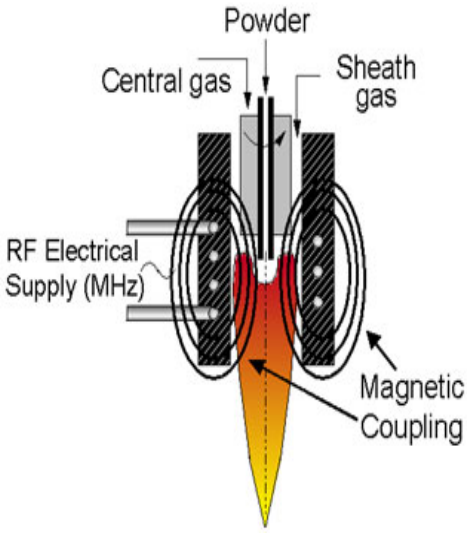

Figure 10. Design of a simple single component rf plasma torch

Design and build rotating-drum splat collector and recirculating flow chamber.

Following the successful integration of aerosol system - rf plasma torch - rf generator, a rotating-drum splat collector and recirculating flow chamber would be designed to be integrated with the system. The plasma torch would be connected with this quench chamber which will be fitted with a water cooled rotating drum. The chemically cleaned, as achieved in Phase 1, B powder will be injected in rf plasma in form of aerosol dispersed in argon and would be melted in the central plasma zone. The molten droplets will be splat quenched on the rotating drum as they hit the water cooled surface and form the phase-pure amorphous Boron. Figure 11 shows the conceptual design of the torch and quench chamber assembly. This fine powder would be collected in the bag house and would go through the jet milling and VI powder separation unit attached to the bag house. The amorphous powder would be collected out while the Argon would be recirculated back into the system.

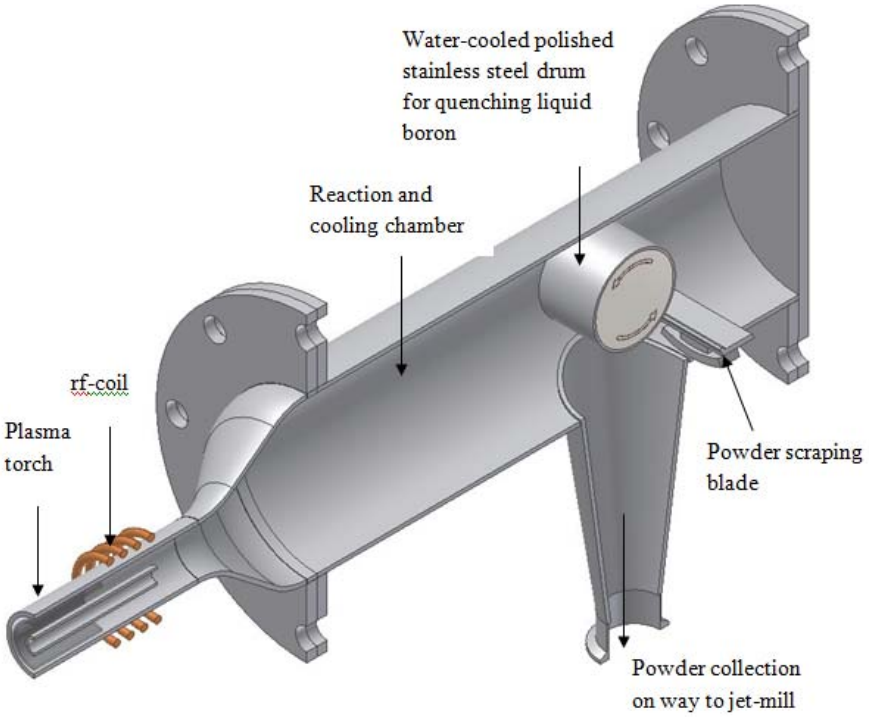

Figure 11. Conceptual design of plasma torch and splat-quench chamber assembly.

Integration of parallel flows to synthesize C-alloyed MgB_2 for high H_{c2}

The ultimate aim of this project is to achieve a manufacturing capability to produce high-performance MgB_2 powder. Our strategy is to achieve this in an rf plasma torch whose input flow is a multi-component aerosol flow containing several ingredient precursor powders. The strategy makes use of two remarkable properties of the flow and temperature characteristics of an rf plasma torch:

- Except near the core of the plasma heating zone the *gas flow is laminar*: each streamline of gas moves through the torch with minimum mixing with adjacent streamlines.
- There is a very strong radial temperature profile in the torch geometry, so that *the temperature reached by each streamline is determined by its radius in the flow*.

We would use the plasma torch as a means of heating several reactant species introduced in the plasma plume as aerosols at different zones. These would be heated to different temperatures and then mixed together in the exhaust plume to initiate non-equilibrium synthesis reactions. By separately controlling the temperature of each reactant it would thereby be possible to vaporize powders of one reactant (Mg and B for our case), and also to heat seed particles such as C nanotubes, or SiC or B_4C nanoparticles, to an optimum substrate temperature for adhesion of the reacting vapors (Figure 12). This control of temperature would lead to the capability which would be unique in the world of synthesis reactions and opens new possibilities.

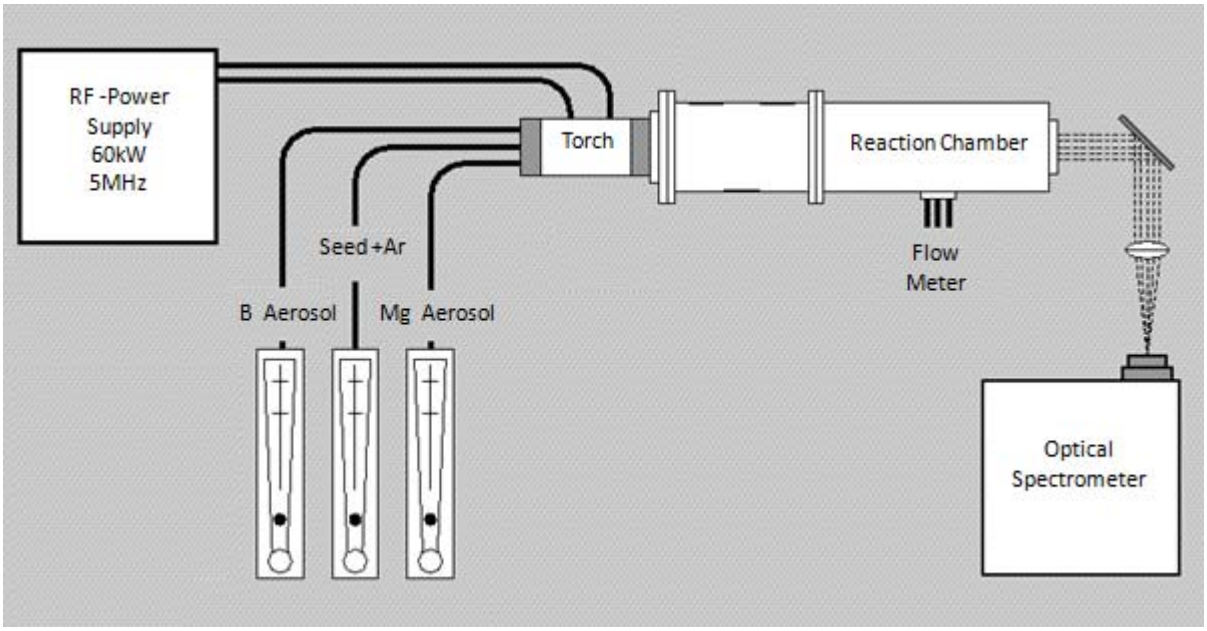

Figure 12. Flow diagram for multi-component rf-plasma synthesis of high-performance doped MgB_2.

Appendix A. Important aspects of the materials science of MgB_2

The importance of pure-amorphous boron to make single-phase MgB_2

Shown in Figure 14 are the variations of transport current with applied field (at 6K and 20K) for 4 different samples of MgB_2 prepared using four different Boron powders namely C98 (Alfa-Aesar, 98% Pure, Crystalline), C99 (FluoroChem, 99% Pure, Crystalline), A9597 (Fluka, 95-97% Pure, Amorphous) and A9999 (Alfa-Aesar, 99.9% Pure, Amorphous). Details of the powders and particle sizes are presented in Table 2 [14]. While Figure 13 shows the microstructures of the resulting MgB_2 made from the above mentioned powders. It is evident from the two figures that the resulting microstructure and transport properties of MgB_2 are highly depended on the starting Boron precursor powder.

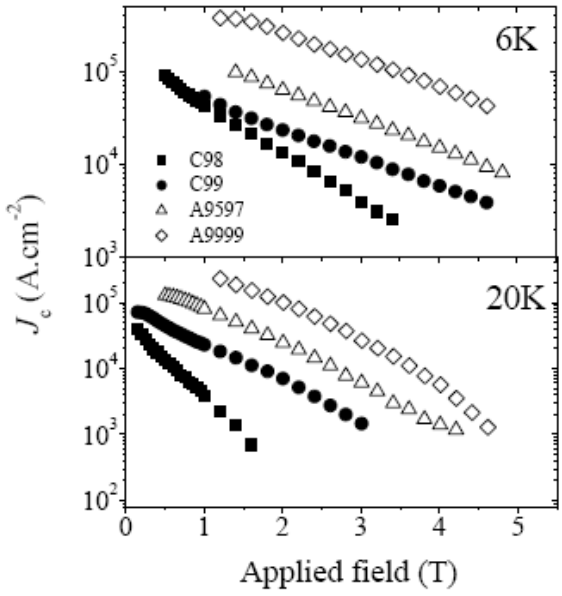

Figure 14. J_c vs. T for MgB_2 samples prepared using four different kinds of boron [12]

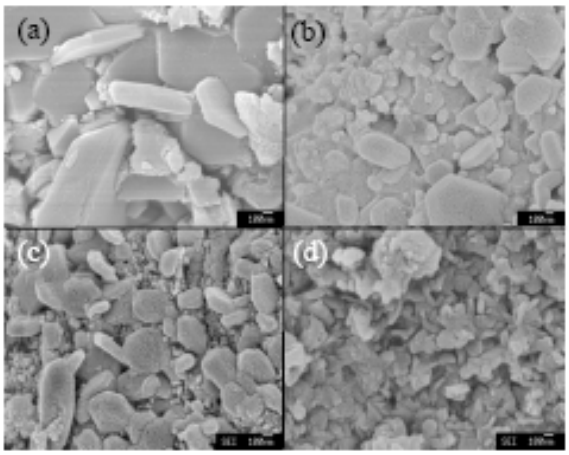

Figure 13. Microstructure of MgB_2 samples prepared using different kinds of boron [12]

Table 2 Specifications for different commercial Boron powders

Boron powder	Source	Form	Purity	Peak value(s) of particle size distribution (μm)
B-C98	Alfa Aesar	Crystalline	98 %	21.10 [325 mesh]
*B-C99	FluoroChem	Crystalline	99 %	11.42, 0.56 [< 40 μm]
*B-A9597	Fluka	Amorphous	95 – 97 %	0.56, 2.42 [-]
B-A9999	Alfa Aesar	Amorphous	99.99%	0.54 [325 mesh]

From the above shown Figure 14 it is clearly seen that MgB_2 samples made from amorphous Boron powder are far superior in the properties as compared to crystalline Boron samples. Even the sample made from less pure amorphous Boron showed better properties than the purer crystalline Boron sample. The exact reason for the fact is though not yet completely understood still one of the possible reasons can be directly related to the fact that as compared to amorphous Boron, the crystalline Boron which is in most of the cases β-rhombohedral has a lower reactivity and allows slower Mg diffusion. Since, the formation reaction of MgB_2 involves inward diffusion of Mg in Boron and reaction at the interface and therefore the above mentioned slow diffusivity and lower reactivity would lead to the formation of leftover intermediate non-superconducting phases in the final product. This has been observed in certain cases.[2, 3, 5].

Commercial amorphous Boron, even-though claimed to be amorphous still contains a small percentage of crystalline phase as shown in the XRD below (Figure 15). ATC, with its rf-plasma synthesis technique proposes to prepare pure nanoscale amorphous Boron.

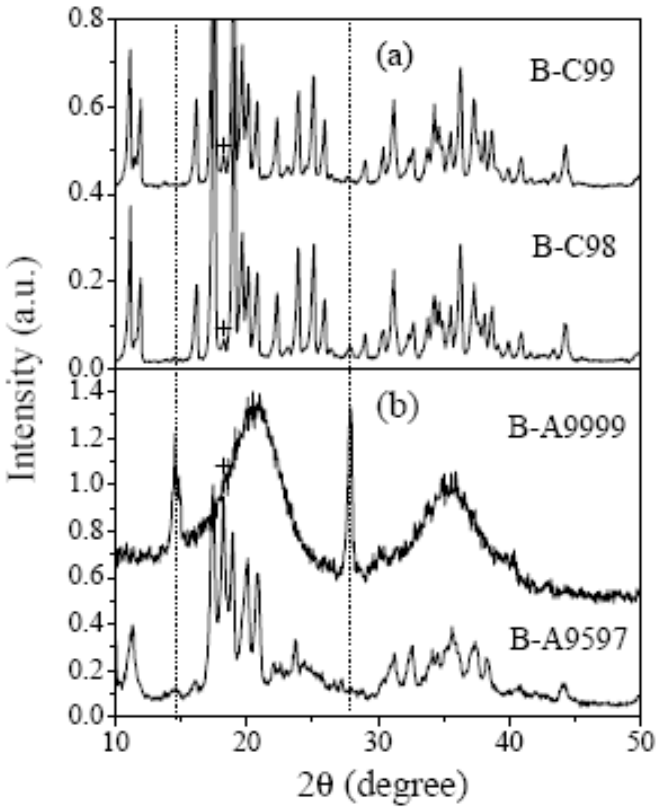

Figure 15. XRD pattern for different kinds of commercial boron powders. Peaks shown with the dotted lines are B_2O_3 phase.

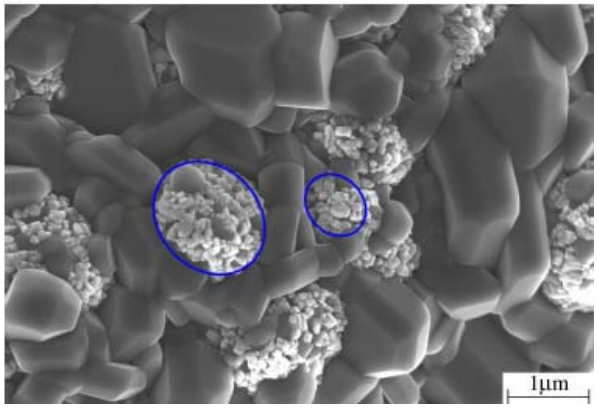

Figure 16. Microstructure of MgB_2 showing insulating MgO on the grain boundaries.

Presence of MgO in starting boron precursor

Another important observed difference between the high performing and mediocre quality MgB_2 superconductors has been the presence of large amount of MgO in the final microstructure. This insulating MgO, shown in blue circles in

Figure 16, resides on the grain boundaries and reduces the effective current carrying cross-section thus limiting the capabilities of the MgB_2 strand[15]. One of the important sources of this very stable MgO is the Boron precursor powder. Most of the Boron powder is prepared by the reduction of B_2O_3 by Mg and hence MgO is a major impurity in final Boron powder (~50% of the total impurity content). ATC, with its proposed plan would be able prepare Boron powder with almost none to very less quantity of MgO impurity phase.

Presence of B_2O_3 in starting Boron precursor

Apart from MgO another major impurity in the commercial Boron is B_2O_3. The presence of this B_2O_3 phase is also detrimental for the reason that during the MgB_2 preparation this B_2O_3 can be reduced by Mg and lead to the formation of the above mentioned MgO phase and therefore removal of B_2O_3 from B is important.

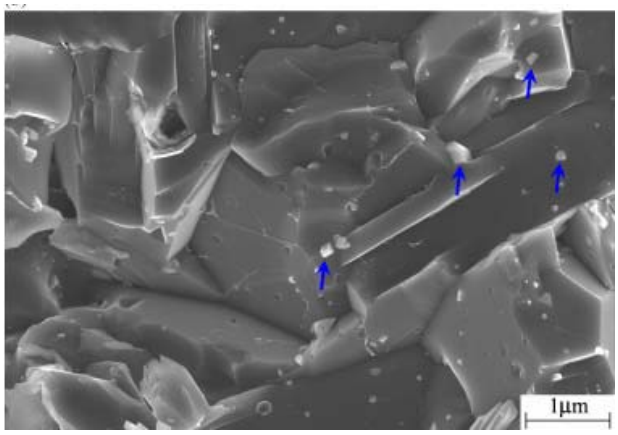

Figure 17. Micrograph of a MgB_2 sample (with very less amount of MgO) [15] prepared in the exact same conditions as Figure 4 but after removing B_2O_3.

Particle (agglomerate) size of starting boron powder

Another important factor affecting the properties of MgB_2 superconducting strands is the starting particle sizes of the precursor powders specially Boron because of the above mentioned fact that MgB_2 is formed by the inward diffusion of Mg in Boron particle followed by the reaction. Therefore, the final grain size of MgB_2 is directly related to the starting Boron particle size as shown in the microstructure in Figure 14. ATC is already commissioning a jet-mill coupled with in-house designed virtual-impactor (two previous projects) which would be used in the final stages of the proposed plan to further reduce the size of Boron powder. It has been shown by various previous research studies that reducing the particle size of starting boron has beneficial effects on the superconducting properties of MgB_2.[16]

References

1. Xu, G.J., et al., *Effect of starting composition and annealing temperature on irreversibility field and critical current density in MgxB2.* Physica C-Superconductivity and Its Applications, 2006. **434**(1): p. 67-70.
2. Giunchi, G., L. Malpezzi, and N. Masciocchi, *A new crystalline phase of the boron-rich metal-boride family: the Mg2B25 species.* Solid State Sciences, 2006. **8**(10): p. 1202.
3. Giunchi, G., et al., *Analysis of the minority crystalline phases in bulk superconducting MgB2 obtained by reactive liquid Mg infiltration.* Physica C-Superconductivity and Its Applications, 2006. **433**(3-4): p. 182-188.
4. Song, X., Journal of Materials Research, 2004. **19**: p. 2245.
5. Yakinci, M.E., et al., *Degradation of superconducting properties in MgB2 by formation of the MgB4 phase.* Journal of Superconductivity, 2002. **15**(6): p. 607-611.
6. Bean, C.P., Rev. Mod. Phys., 1964. **36**: p. 31.
7. Caplin, A.D., et al., *Critical fields and critical currents in MgB2* Superconductor Science & Technology, 2003. **16**: p. 176-182.
8. Wilke, R.H.T., et al., *Synthesis of Mg(B1-xCx)(2) powders.* Physica C-Superconductivity and Its Applications, 2005. **432**(3-4): p. 193-205.
9. Ohmichi, E., et al., *Enhancement of the Irreversibility Field by Carbon Substitution in Single Crystal MgB2* Journal of Physical Society of Japan. 73 2004. **73**: p. 2065.
10. Braccini, V., et al., *High-field superconductivity in alloyed MgB2 thin films (vol 71, pg 012504, 2005).* Physical Review B, 2005. **71**(17).
11. Mellado-Gonzalez, J.P., *Development of a chemical kinetics model for inductive plasma simulations.* VKI SR, 1998. **36**.
12. Bernardi, D., et al., *Three-dimensional effects in the modelling of ICPTs.* The European Physical Journal D, 2003. **25**: p. 271-277.
13. Bernardi, D., et al., *Three-dimensional modelling of inductively coupled plasma torches.* The European Physical Journal D, 2002. **22**: p. 119-125.
14. Chen, S.K., et al., *Strong influence of boron precursor powder on the critical current density of MgB2.* Superconductor Science & Technology, 2005. **18**(11): p. 1473-1477.
15. Jiang, J., et al., *Influence of boron powder purification on the connectivity of bulk MgB2.* Superconductor Science & Technology, 2006. **19**(8): p. L02.
16. Xu, X., et al., *Influence of ball-milled low purity boron powder on the superconductivity of MgB2.* IEEE Transactions on Applied Superconductivity, 2007. **17**(2): p. 2782-2785.